Electronic Supplementary Information

Exciplex-induced TADF, persistent RTP and ML in a host-guest doping system

Yunsheng Wang,[a,b] Mingxue Gao,[a] Jia Ren,[a] Jiayi Liang,[a] Yao Zhao,[a] Manman Fang,[a] Jie Yang,[a,*] Zhen Li[a,b,c,d,*]

[a,] Institute of Molecular Aggregation Science, Tianjin University, Tianjin, 300072, China. Email: jieyang2018@tju.edu.cn; lizhen@whu.edu.cn.

[b,] Joint School of National University of Singapore and Tianjin University, International Campus of Tianjin University, Binhai New City, Fuzhou, 350207, China.

[c,] Department of Chemistry, Wuhan University, Wuhan, 430072, China.

[d,] Wuhan National Laboratory for Optoelectronics, Huazhong University of Science and Technology, Wuhan 430074, China.

Methods

Syntheses

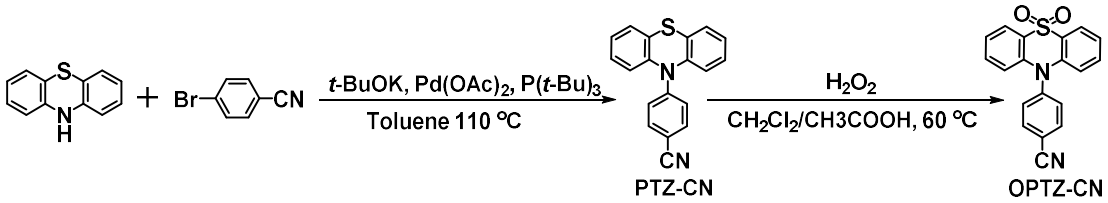

Scheme S1 The synthetic route of PTZ-CN and OPTZ-CN.[1]

PTZ-CN: Phenothiazine (1.99 g, 10 mmol), 4-bromobenzonitrile (1.82 g, 10 mol), potassium tert-butoxide (1.68 g, 15 mmol), palladium acetate (0.11 g, 0.5 mmol) and tri-tert-butylphosphine solution (0.5 mL, 0.25 mmol) were dissolved in toluene (100 mL) in a Schlenk tube. The resultant mixture was refluxed for 12 hours under argon, then extracted with dichloromethane. The combined organic extracts were dried over anhydrous Na_2SO_4 and concentrated by rotary evaporation. The crude product was purified by column chromatography on silica gel using petroleum ether/dichloromethane (3:1 v/v) as eluent to afford a white solid in the yield of 50%. ^{1}H-NMR (400 MHz, $CDCl_3$) δ(ppm): (ppm): 7.42-7.49 (m, 4H), 7.26-7.31 (m, 4H), 7.18-7.22 (m, 2H), 7.05-7.07 (m, 2H). ^{13}C-NMR (100 MHz, $CDCl_3$) δ(ppm): 149.0, 141.0, 133.6, 133.1, 128.9, 127.4, 126.2, 125.9, 119.5, 116.8. MS (EI), m/z: 300.03 ([M^+], calcd for $C_{19}H_{12}N_2S$, 300.07. Anal. Calcd for $C_{19}H_{12}N_2S$: C, 75.97; H, 4.03; N, 9.33; S 10.67. Found: C, 76.21; H, 3.93; N, 9.29; S, 10.65.

OPTZ-CN: PTZ-CN (1.33 g, 4 mmol) was dissolved in dichloromethane (90 mL), acetic acid (45 mL) and H_2O_2 (2 mL). After reacting for another 24 hours at 60 ºC, the reaction mixture was extracted with dichloromethane and further purified by column chromatography using petroleum ether/ethyl acetate (8:1 v/v) as eluent to afford a white solid in the yield of 80%.^{1}H-NMR (400 MHz, $CDCl_3$) δ(ppm): (ppm): 8.18-8.20 (d,

2H), 8.02-8.04 (d, 2H), 7.57-7.59 (d, 2H), 7.40-7.45 (t, 2H), 7.26-7.32 (m, 2H), 6.52-6.54 (d, 2H). ^{13}C-NMR (100 MHz, $CDCl_3$) δ (ppm): 143.1, 140.1, 135.2, 133.0, 132.0, 123.8, 123.3, 122.7, 117.5, 116.7, 114.2. HRMS (EI), m/z: 355.0521 ($[M+Na]^+$, calcd for $C_{19}H_{12}N_2SNa$, 355.0517.

M-CN crystal: The M-CN crystal was prepared by the slow solvent evaporation method. 99.0 mg of OPTZ-CN and 1.0 mg of PTZ-CN were dissolved in 3.0 mL of dichloromethane (DCM), transferred to a vial and capped. Standing at room temperature and crystals were obtained after solvent evaporation.

Characterization

^{1}H NMR spectra and ^{13}C NMR spectra were recorded on a 400 MHz Bruker Ascend spectrometer. Mass spectra were measured on a ZAB 3F-HF mass or UHPLC/Q-TOF MS spectrophotometer. Elemental analyses of carbon, hydrogen, nitrogen and sulfur were measured on a Perkin-Elmer microanalyzer. UV-Vis spectra were measured on Shimadzu UV-2600. Photoluminescence spectra and long RTP lifetimes were performed on a Hitachi F-4600 fluorescence spectrophotometer. Powder X-ray diffraction (PXRD) patterns were recorded by Rigaku Smartlab9KW. The single-crystal X-ray diffraction data were collected in XtaLAB SuperNova X-ray diffractometer or Bruker APEX-II CCD diffractometer. Photoluminescence quantum yields and lifetimes were determined with FLS1000 spectrometer.

The Gaussian 09 program was utilized to perform the calculations. The ground state (S_0) geometry of OPTZ-CN dimer was obtained from the single crystal structures and no further geometry optimization was conducted in order to maintain the specific molecular configurations and corresponding intermolecular locations. The ground state (S_0) geometry of OPTZ-CN/PTZ-CN was optimized based on m062x/6-31g*.

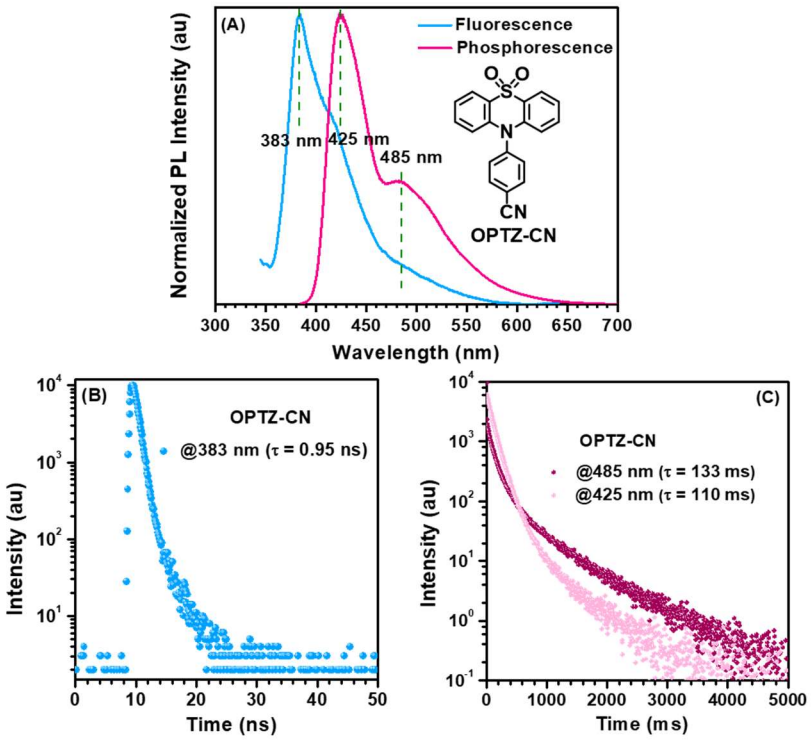

Figure S1 (A) Normalized fluorescence and phosphorescence spectra of OPTZ-CN crystal at room temperature; **(B)** Fluorescence decay curve of OPTZ-CN crystal at 383 nm; **(C)** RTP decay curves of OPTZ-CN crystal at 485 and 428 nm.

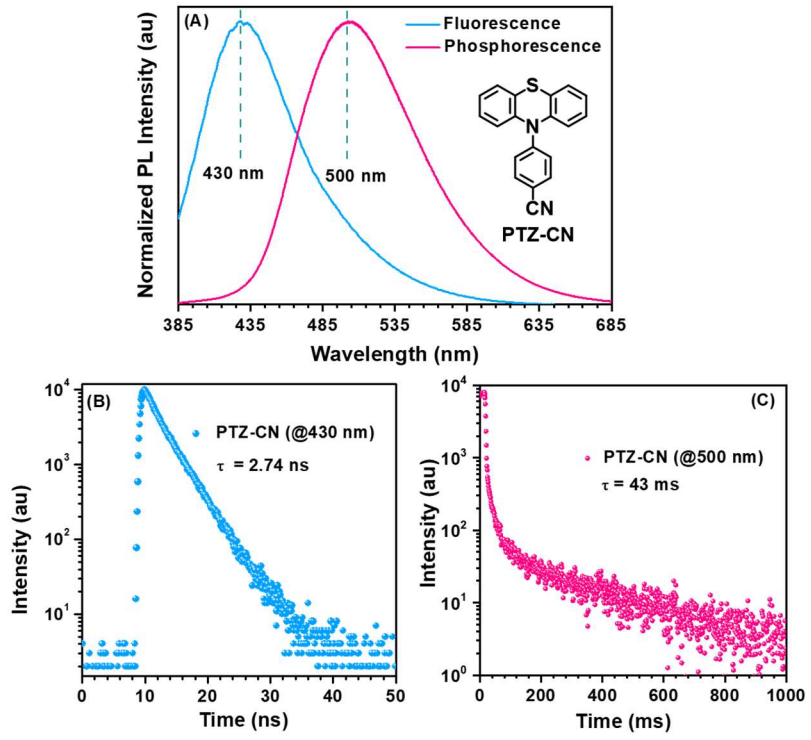

Figure S2 (A) Normalized fluorescence and phosphorescence spectra of PTZ-CN crystal at room temperature; **(B)** Fluorescence decay curve of PTZ-CN crystal at 430 nm; **(C)** RTP decay curve of PTZ-CN crystal at 500 nm.

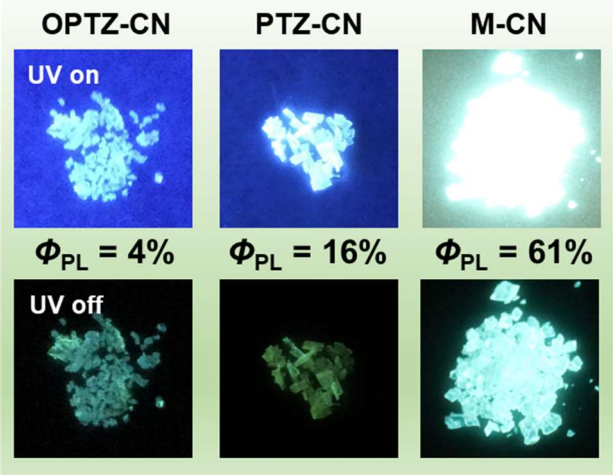

Figure S3 Luminescent photos of OPTZ-CN, PTZ-CN and M-CN crystals under 365 nm UV on and UV off states.

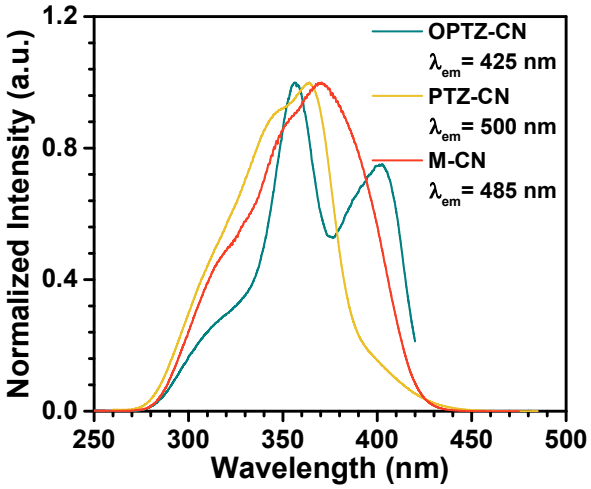

Figure S4 The phosphorescence excitation spectra of OPTZ-CN, PTZ-CN and M-CN.

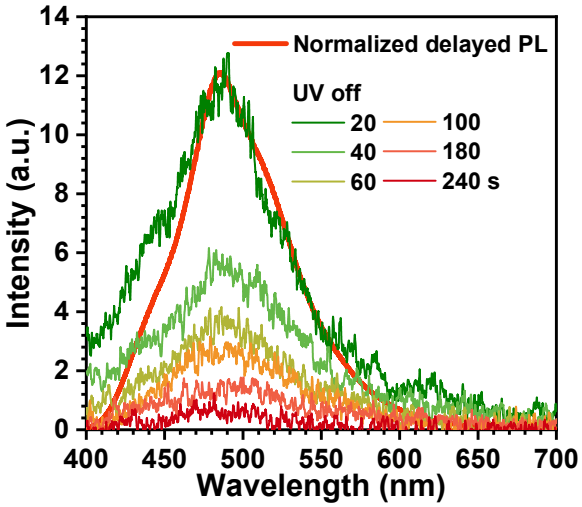

Figure S5 Time-resolved PL spectra of M-CN.

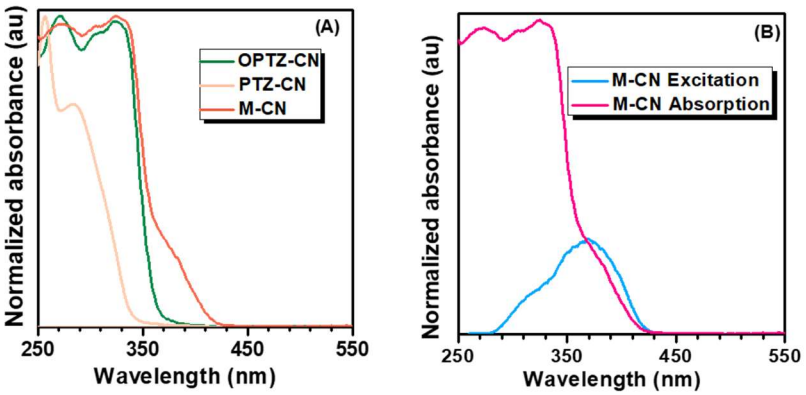

Figure S6 (A) Normalized UV-Vis absorption spectra of OPTZ-CN crystal, PTZ-CN solution and M-CN crystal; **(B)** Normalized UV-Vis absorption spectrum of M-CN crystal and its excitation spectrum for the emission band at 485 nm.

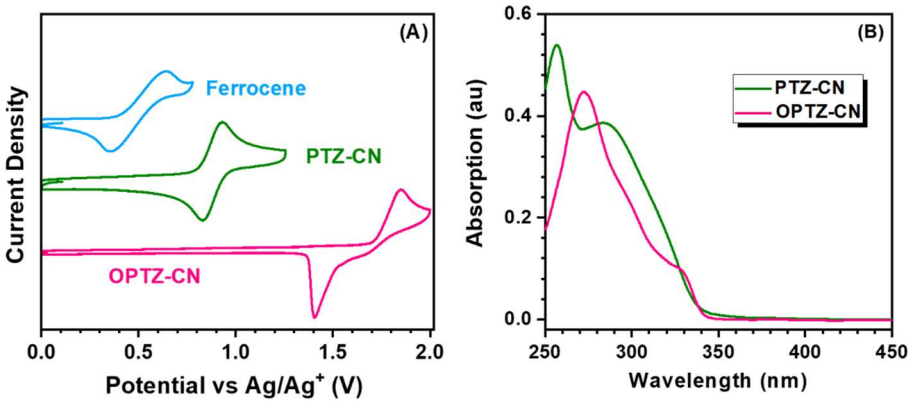

Figure S7 (A) Cyclic voltammetry (CV) curves of ferrocene, PTZ-CN and OPTZ-CN in CH_2Cl_2 solution with n-Bu_4NPF_6 supporting electrolyte (CV measurements were performed using a three-electrode configuration consisting of a glassy carbon working electrode, a glassy carbon counter electrode and an $Ag/AgNO_3$ as a reference electrode); **(B)** Normalized UV-Vis absorption spectra of PTZ-CN and OPTZ-CN in CH_2Cl_2 solution (concentration: 10^{-5} M).

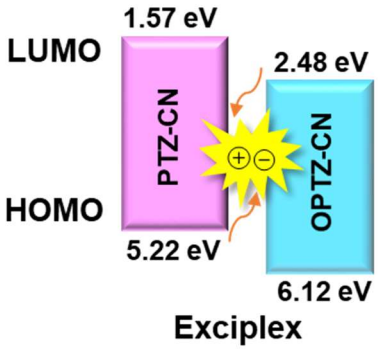

Figure S8 Exciplex based on OPTZ-CN (acceptor) and PTZ-CN (donor), and their energy levels of HOMO/LUMO.

Table S1 The emission lifetimes of M-CN crystal at different temperatures.

Temperature (K)	**τ (ms)**, λ_{ex} = 365 nm, λ_{em} = 478 nm	**τ (ms)**, λ_{ex} = 365 nm, λ_{em} = 510 nm
100	58.18	58.22
120	58.09	57.82
150	57.30	57.27
180	56.68	56.41
210	55.81	55.27
250	52.32	52.31
280	45.44	45.17
300	37.13	36.90
330	21.79	21.12
360	9.54	9.28

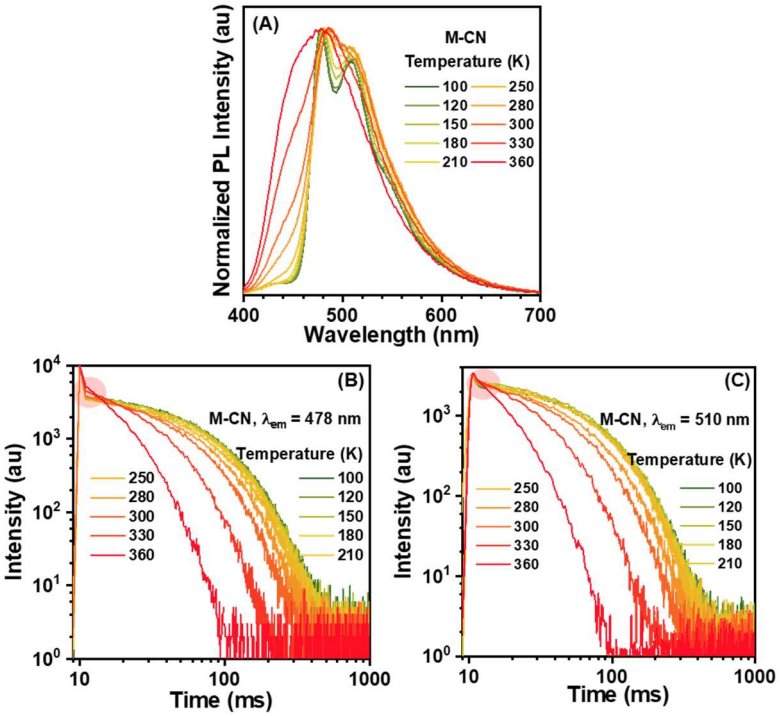

Figure S9 (A) Normalized steady-state PL spectra of M-CN crystal at different temperatures; **(B)** PL decay curves at 478 nm for M-CN crystal at different temperatures; **(C)** PL decay curves at 510 nm for M-CN crystal at different temperatures.

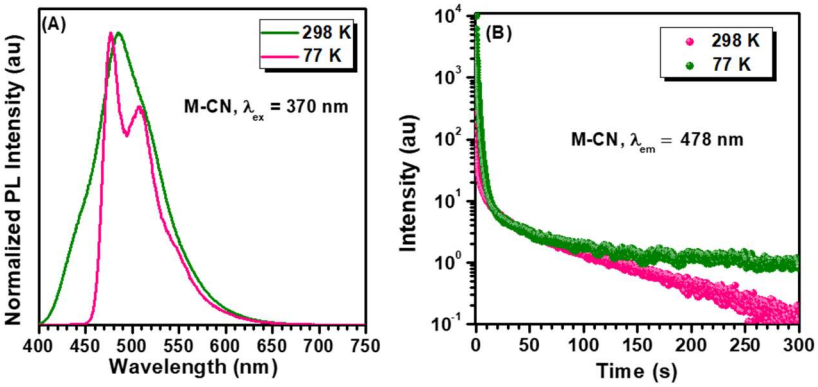

Figure S10 (A) Normalized delayed PL spectra of M-CN crystal at 298 and 77 K; **(B)** Phosphorescence-decay curves of M-CN crystal at 298 and 77 K.

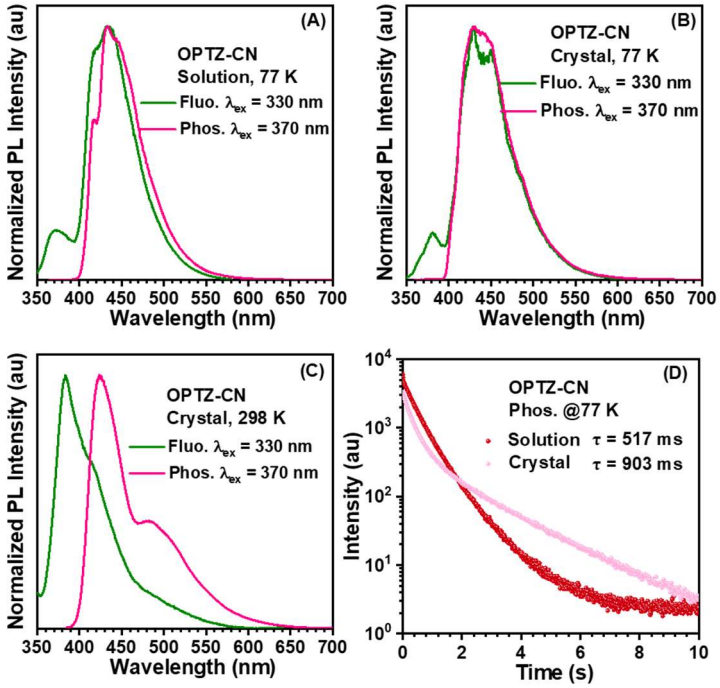

Figure S11 (A) Normalized fluorescence and phosphorescence spectra of OPTZ-CN solution at 77 K (concentration: 10^{-5} M); **(B)** Normalized fluorescence and phosphorescence spectra of OPTZ-CN crystal at 77 K; **(C)** Normalized fluorescence and phosphorescence spectra of OPTZ-CN crystal at 298 K; **(D)** Phosphorescence decay curves of OPTZ-CN solution and crystal at 77 K.

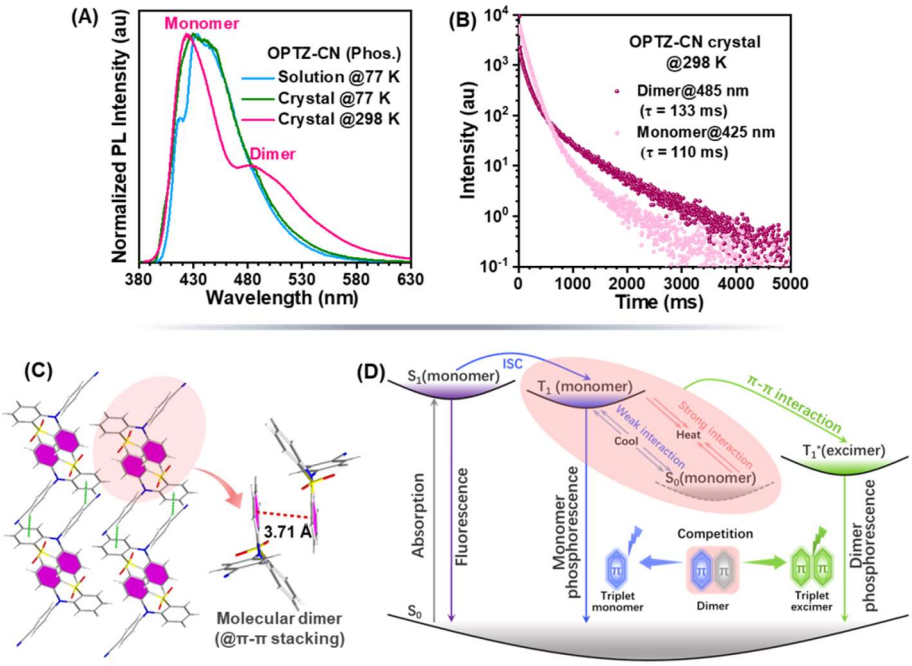

Figure S12 (A) Normalized phosphorescence spectra of OPTZ-CN solution at 77 K, OPTZ-CN crystal at 77 and 298 K; **(B)** RTP decay curves of OPTZ-CN crystal at 485 and 425 nm; **(C)** Single crystal structure of OPTZ-CN; **(D)** Proposed mechanism of the RTP behavior of OPTZ-CN crystal.

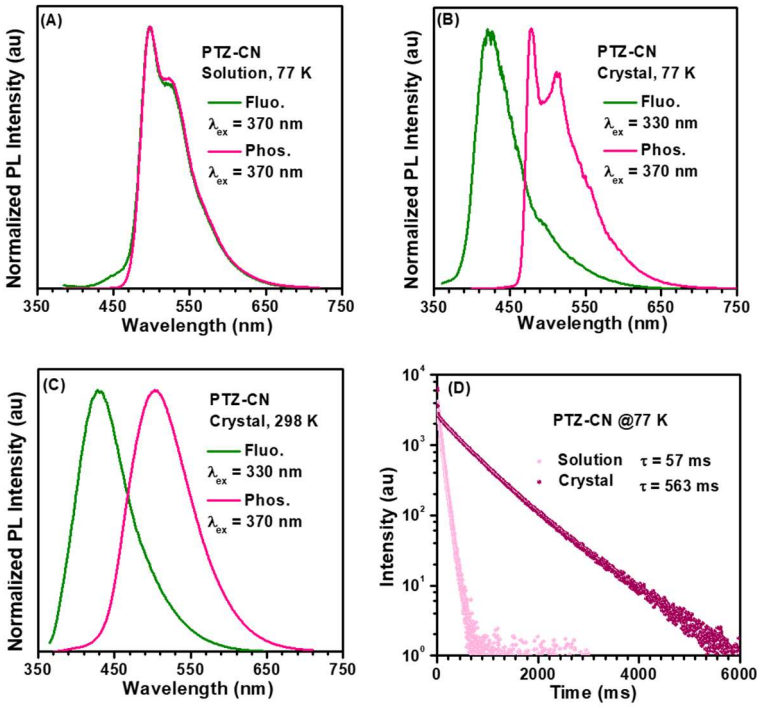

Figure S13 (A) Normalized fluorescence and phosphorescence spectra of PTZ-CN solution at 77 K (concentration: 10^{-5} M); **(B)** Normalized fluorescence and phosphorescence spectra of PTZ-CN crystal at 77 K; **(C)** Normalized fluorescence and phosphorescence spectra of PTZ-CN crystal at 298 K; **(D)** Phosphorescence decay curves of PTZ-CN solution and crystal at 77 K.

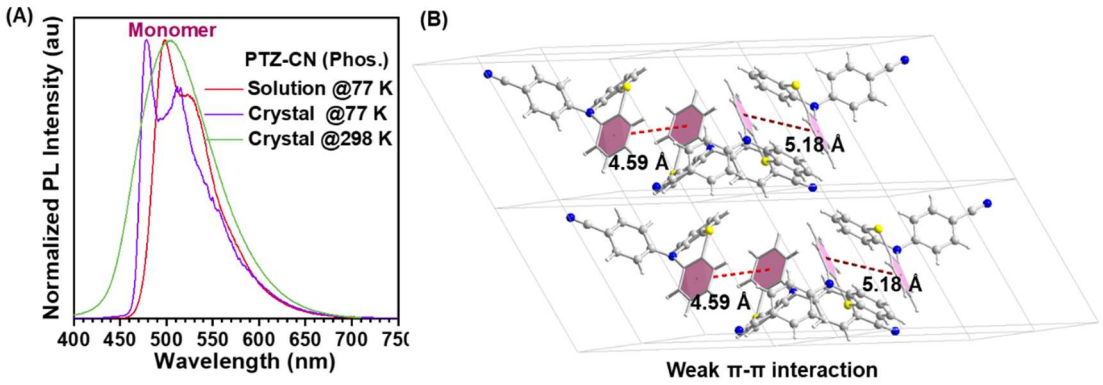

Figure S14 (A) Normalized phosphorescence spectra of PTZ-CN solution at 77 K, OPTZ-CN crystal at 77 K and 298 K; **(B)** Single crystal structure of PTZ-CN.

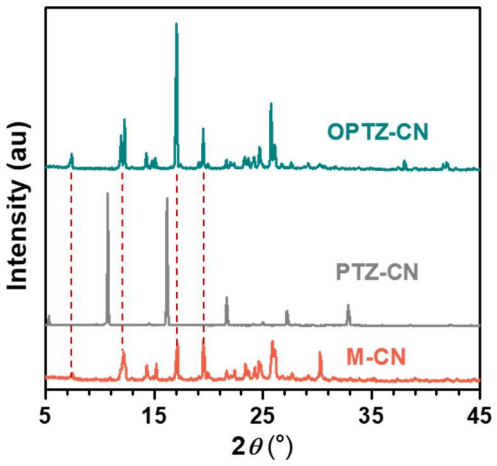

Figure S15 PXRD patterns of OPTZ-CN, PTZ-CN and M-CN powders.

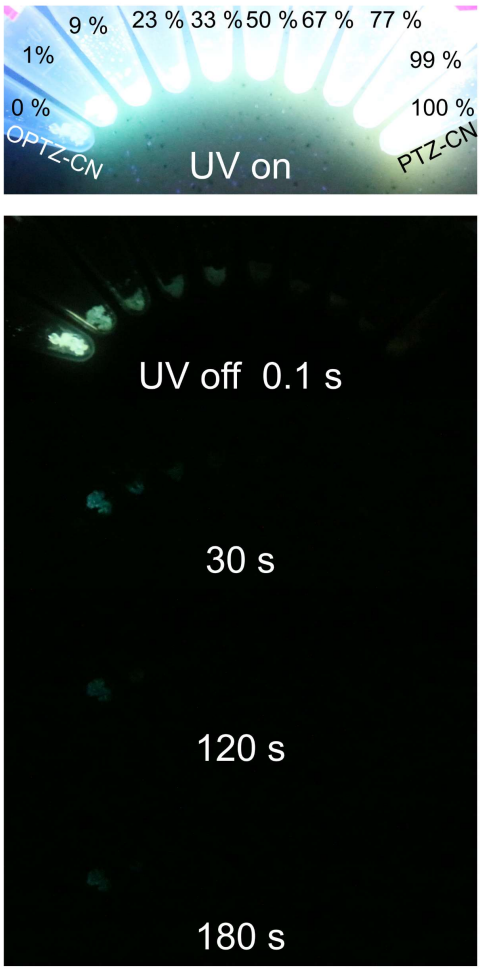

Figure S16 Afterglow photographs of M-CN samples containing different mass ratios of PTZ-CN.

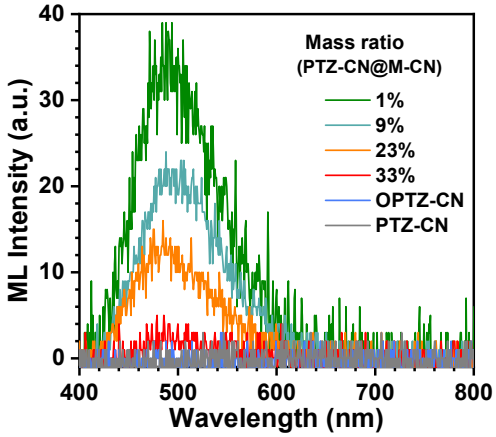

Figure S17 ML spectra of M-CN crystals with different ratios of PTZ-CN.

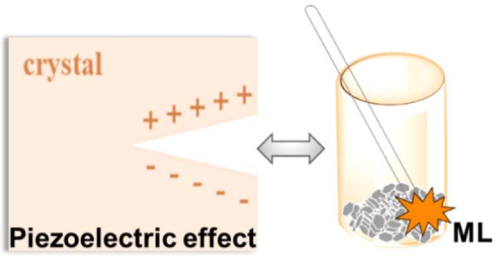

Figure S18 Schematic diagram of ML induced by piezoelectric effect.

Table S2 The single crystal data for OPTZ-CN, PTZ-CN and M-CN.

Crystal	OPTZ-CN	PTZ-CN	M-CN
Formula	$C_{19}H_{12}N_2O_2S$	$C_{19}H_{12}N_2S$	$C_{19}H_{12}N_2O_2S$
Wavelength (Å)	0.71073	0.71073	1.54184
Space Group	P-1	P -1	P -1
Cell Lengths (Å)	a=8.2330(16) b=8.8726(17) c=12.131(2)	a= 10.3472(10) b= 12.6805(12) c= 12.7346(12)	a=8.2579(4) b=8.8946(4) c=12.1498(5)
Cell Angles (°)	α= 95.547(3) β= 96.437 (3) γ= 114.746(2)	α= 91.2810(14) β= 109.3896(14) γ= 111.0594(13)	α= 95.502(3) β= 96.531(4) γ= 114.779(4)
Cell Volume ($Å^3$)	789.5	1451.7(2)	794.73(7)
Z	2	4	2
Density (g/cm^3)	1.389	1.374	1.389
F(000)	344.0	624.0	344.0
h_{max}, k_{max}, l_{max}	10,11,16	12,15,15	9,10,14
CCDC number	2235978	2216826	2216776

References

S1. Borowicz, P.; Herbich, J.; Kapturkiewicz, A.; Opallo, M.; Nowacki, J. Radiative and nonradiative electron transfer in donor-acceptor phenoxazine and phenothiazine derivatives. *Chem. Phys*., 1999, **249**, 49-62.